

## Research Article

# A Novel Heat Sink Design and Prototyping for LED Desk Lamps

Li-Ming Chu,<sup>1</sup> Wei-Chin Chang,<sup>1</sup> and Ting Hsuan Huang<sup>2</sup>

<sup>1</sup>Department of Mechanical Engineering, Southern Taiwan University of Science and Technology, Tainan City 71005, Taiwan

<sup>2</sup>Department of Mechanical and Automation Engineering, I-Shou University, Kaohsiung City 84001, Taiwan

Correspondence should be addressed to Wei-Chin Chang; [wchang@mail.stust.edu.tw](mailto:wchang@mail.stust.edu.tw)

Received 28 September 2014; Accepted 16 January 2015

Academic Editor: Mo Li

Copyright © 2015 Li-Ming Chu et al. This is an open access article distributed under the Creative Commons Attribution License, which permits unrestricted use, distribution, and reproduction in any medium, provided the original work is properly cited.

Light-emitting diode (LED) is a modern lighting device. If the heat dissipating mechanism of LED desk lamp is not well designed, the induced high temperature will cause the reduction of illumination and life time of lamp. Therefore, the heat sink design becomes a key technology for LED lighting device. This study developed a methodology to design and analyze a heat sink for LED cooling. Four different types of heat sinks with fins in longitudinal or transverse directions and with or without vents on the base plate were compared. By using the CFD software FLUENT, heat flux and temperature around the heat sink were analyzed, and the surface temperature distribution was also investigated. The simulation outcomes were compared with experiments results to verify analysis accuracy. The comparisons show only slight differences, and the deviations were less than 4.0%. For cooling LED desk lamp, the design of using 12 vents on both sides of heat sink through natural convection to create the chimney effect was adopted; consequently, the temperature dropped 5°C in average. This design can also reduce the material of heat sink, LED lamp weight, and production cost.

## 1. Introduction

Traditional incandescent lamps are energy consuming devices with high heat emitting rate. For a 100 W incandescent lamp, 12% consumed energy is converted into heat, 83% energy becomes infrared radiation, and only 5% turns to visible light. In contrast, for a light-emitting diode, so called LED, 15% to 30% consumed energy is converted into visible light, and the rest becomes heat. In recent years, due to the rising awareness of environmental issue, the high luminous efficiency LED, contributed by low power consumption and long life time, has great potential for lighting application.

A higher power LED produces relatively more heat, which makes heat dissipation become very important. There are many popular heat dissipating devices, such as heat pipe, heat sink, and fan. To most LED devices, heat sink is favored. The cooling fins design of heat sink will affect the LED luminous efficiency. This study developed a technology to design high efficiency heat sink for LED desk lamp.

The use of LED lighting is a trend of the future; there are many research works focusing on heat releasing problems of

LED. Most input energy of high power LED turns to heat; if it fails to effectively discharge the waste heat generated by the current (Joule's law), it will make the temperature at the junction of LED chip become too high and consequently decrease the luminous efficiency and life-time of LED [1, 2].

Shaukatullah et al. [3] studied the optimal design of pin fin at low flow rates; the results showed that, with 6 × 6 cylindrical aluminum fins on a 25 mm × 25 mm base plate, a better cooling effect can be achieved by using 15 mm high pins with 1.5 × 1.5 mm cross section at 1 m/s flow rate of air.

De Lieto Vollaro et al. [4] studied a finned plate in natural convection circumstance; they used a simplified relation of fins efficiency to present a process to optimize the fin spacing. The results showed that, with such simple model to calculate the heat transfer of fins, the temperature variation and end effects in the vertical direction can be neglected, and the finite fin conductivity reduced the optimal fin spacing. Chuang et al. [5] analyzed the cooling fins of high power LED, in order to apply LED to the liquid crystal display. The experiments were done in constant temperature environment, and the temperatures of cooling fins were measured. CFD simulation

was then conducted with four concerned parameters, which were the thickness of the fin base, fin height, fin thickness, and the interval of fin. The simulation results were verified with the experiments data. Finally, with the Taguchi method, the optimal shape of the fin was decided.

NICHIA Corp. [6] pointed out that the maximum temperature of LED configuration normally happens at the PN junction, so the junction temperature is an important parameter for LED design, and it can be obtained by the introduction of the concept of "thermal resistance." Theoretically, under constant power consumption and the same ambient temperature condition, the greater the thermal resistance, the larger the value of junction temperature, which implied poor cooling effect. In spite of using practical measurements or theoretical analysis to obtain the thermal resistance of the heat sink components, it is important for designing electronic products. Tian et al. [7] investigated the heat dissipating condition of high power LED with different kinds of heat sinks. A simplified model of LED was introduced with two resistances; one is the resistance between the die junction and the top, and the other is the resistance between the die junction and the printed circuit board (PCB). In addition to the PCB and lamp body models, the thermal model of LED lamp was built.

Harahap and Setio [8] investigated five different types of cooling fins through experiments by changing the fin spacing, length, and thickness. With nondimensional parameters formulated by similarity analysis, the results showed that the fin spacing and length were the main parameters to affect the cooling effect. Narasimhan and Majdalani [9] explored the performance of the plate-fin and cylindrical fin in natural convection through a CFD software. They successfully used a compact heat sink model to reduce the number of grids and computing time but still accurately presented the entrance temperature and velocity distribution.

This work developed an analysis technology for designing the heat sink of LED lamp, which is suitable for LED lamp manufacturers to design cooling fins for heat dissipation. In the early design stage, CAD was used to design the heat sink of LED lamp and then to using computer graphics software to construct the grid pattern inside the fins. Natural convection was adopted as the movement of surrounding air without considering the influence of radiation [10, 11]. Measured heat flux data from experiments were applied as boundary conditions in the simulation model, a commercial software FLUENT was used to analyze flow field and temperature field around the cooling fins, and temperatures from different positions of fin were acquired to confirm the relevance of design concept.

## 2. Theoretical Analysis

**2.1. Governing Equation.** The heat convection condition in this study was considered as a three-dimensional incompressible flow; the process was assumed to be in steady state. For momentum equations, the working fluid is air, and density changes with temperature. The solving equations can be expressed as follows.

Continuity equation is as follows:

$$\frac{\partial(\rho u)}{\partial x} + \frac{\partial(\rho v)}{\partial y} + \frac{\partial(\rho w)}{\partial z} = 0. \quad (1)$$

The momentum equation in  $X$  direction is as follows:

$$u \frac{\partial u}{\partial x} + v \frac{\partial u}{\partial y} + w \frac{\partial u}{\partial z} = -\frac{1}{\rho} \frac{\partial P}{\partial x} + \nu \frac{\partial^2 u}{\partial x^2} + \frac{\partial^2 u}{\partial y^2} + \frac{\partial^2 u}{\partial z^2}. \quad (2)$$

The momentum equation in  $Y$  direction is as follows:

$$u \frac{\partial v}{\partial x} + v \frac{\partial v}{\partial y} + w \frac{\partial v}{\partial z} = -\frac{1}{\rho} \frac{\partial P}{\partial y} + \nu \frac{\partial^2 v}{\partial x^2} + \frac{\partial^2 v}{\partial y^2} + \frac{\partial^2 v}{\partial z^2}. \quad (3)$$

The momentum equation in  $Z$  direction is as follows:

$$u \frac{\partial w}{\partial x} + v \frac{\partial w}{\partial y} + w \frac{\partial w}{\partial z} = -\frac{1}{\rho} \frac{\partial P}{\partial z} + \nu \frac{\partial^2 w}{\partial x^2} + \frac{\partial^2 w}{\partial y^2} + \frac{\partial^2 w}{\partial z^2} + g\beta(T - T_{\infty}). \quad (4)$$

Energy conservation equation is as follows.

Object in 3-dimensional space is as follows:

$$\rho C \frac{\partial T}{\partial t} = k \left( \frac{\partial^2 T}{\partial x^2} + \frac{\partial^2 T}{\partial y^2} + \frac{\partial^2 T}{\partial z^2} \right) + Q. \quad (5)$$

Working fluid is as follows:

$$u \frac{\partial T}{\partial x} + v \frac{\partial T}{\partial y} + w \frac{\partial T}{\partial z} = \alpha \left( \frac{\partial^2 T}{\partial x^2} + \frac{\partial^2 T}{\partial y^2} + \frac{\partial^2 T}{\partial z^2} \right), \quad (6)$$

wherein  $u$ ,  $v$ , and  $w$  represent  $x$ ,  $y$ , and  $z$  direction of velocity vector,  $\rho$  is the fluid density,  $P$  and  $T$  are the fluid pressure and temperature, respectively,  $\nu$  is the dynamic viscosity coefficient,  $g$  is the gravitational acceleration,  $\beta$  is the thermal expansion coefficient of the fluid,  $T_{\infty}$  is the ambient temperature,  $C$  is the specific heat of the object,  $k$  is the thermal conductivity of object,  $Q$  is the power output of the heat source, and  $\alpha$  is the thermal diffusivity.

In natural convection, Rayleigh number is used to classify the laminar flow and turbulent flow.  $R_a$  is expressed as

$$R_{a_L} = Gr_L Pr = \frac{gL^3 \beta (T_j - T_{\infty})}{\nu^2}, \quad (7)$$

wherein  $g$  is the gravitational acceleration,  $L$  is the length of the heat sink,  $\beta$  is the thermal expansion coefficient of the fluid,  $T_j$  is average temperature of the LED chip connectors,  $T_{\infty}$  is the ambient temperature,  $\nu$  is the coefficient of dynamic viscosity,  $\alpha$  is the thermal diffusivity, and  $Gr$  is the ratio of buoyancy force to viscous force.  $R_a < 10^9$  means laminar flow, and  $R_a > 10^9$  is turbulent flow.

**2.2. Boundary Conditions.** In this study, the output boundary of CFD analysis was assumed to be a pressure outlet. The heat sources are nine 1 W LEDs, and the radiant heat was ignored. Cooling fins and base plate were made of aluminum. The ambient temperature was 20°C; the air properties at 20°C are shown in Table 1.

TABLE 1: Properties of air at 20°C.

Thermal Conductivity (W/m·k)	0.0257
Specific heat (kJ/kg·K)	1005
Density (kg/m <sup>3</sup> )	1.205
Viscosity (m <sup>2</sup> /s)	$1.511 \times 10^{-5}$
Coefficient of thermal expansion (1/K)	$3.43 \times 10^{-3}$



FIGURE 1: Type 1 heat sink.



FIGURE 2: Drawing of type 2 heat sink.

**2.3. Flow Field Assumption.** Through the calculation of (7), the studied fluid was laminar flow. Most LEDs were considered to dissipate heat with natural convection; this idea was also adopted in this work. Because the density changes with the temperature, the buoyancy force cannot be neglected. The ambient temperature was 20°C (293 K), the working fluid was the incompressible air, and the boundary between fluid and wall was in no-slip condition.

### 3. The Experimental Setup

**3.1. Heat Sink Configuration Design.** Four different types of cooling heat sinks were compared. Type 1 with longitudinal fins (Figure 1), type 2 with transverse fins (Figure 2), type 3 with longitudinal fins and cooling holes (Figure 3), and type 4 with transverse fins and cooling holes (Figure 4).

**3.2. Desk Lamp.** The aluminum cooling heat sink was made as a base plate, and nine 1 W white LEDs were installed on the plate to form a desk lamp, as shown in Figure 5.

**3.3. Environment Control and Monitor Points.** To be consistent with the simulation condition, the tested object was placed in a controlled environment with a thermostat to adjust air conditioner for maintaining the ambient temperature at 20°C. When heat sink reached steady state, unnecessary disturbance in the flow field was avoided to ensure the consistency of experimental and simulation environments. Three temperature monitoring points on the heat sink were chosen as shown in Figure 6.

**3.4. Error Analysis.** This study used numerical simulation to analyze the cooling efficiencies of different types of heat sinks, and the accuracies were verified with experiment data.



FIGURE 3: Type 3 heat sink.



FIGURE 4: Type 4 heat sink.



FIGURE 5: Nine 1 W white LEDs installed on the aluminum base plate.

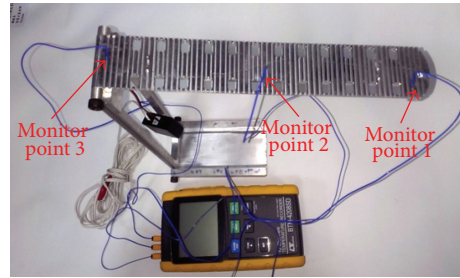


FIGURE 6: Monitor points.

The error analysis was calculated as follows:

$$\text{Deviation value} = \frac{|T_{\text{experiment}} - T_{\text{simulation}}|}{T_{\text{experiment}}} \quad (8)$$

### 4. Results and Discussions

GAMBIT was used to construct mesh of heat sinks (type 1~4) as shown in Figures 7(a)~7(d), and then FLUENT was applied to visualize the velocity and temperature fields.

Figure 8(a) shows the air velocity distribution around type 1 heat sink under 20°C ambient temperature. Due to larger contact areas, both ends of type 1 fin have higher heat dissipating efficiencies; hence the fastest velocity of air flow (about 0.0553 m/s) located at the front and rear ends. Figure 8(b) displays the temperature distribution of type 1 heat sink, which shows that lower temperatures occurred in the front and rear ends of heat sink, and higher temperatures were in the middle area. Figures 8(a) and 8(b) indicate that faster air velocity happened at lower temperature area. The maximum overall temperature of table lamp in steady-state condition is 50.91°C. The experimental results are shown in Table 2; the maximum deviation between experiment and simulation results is 2.1%.

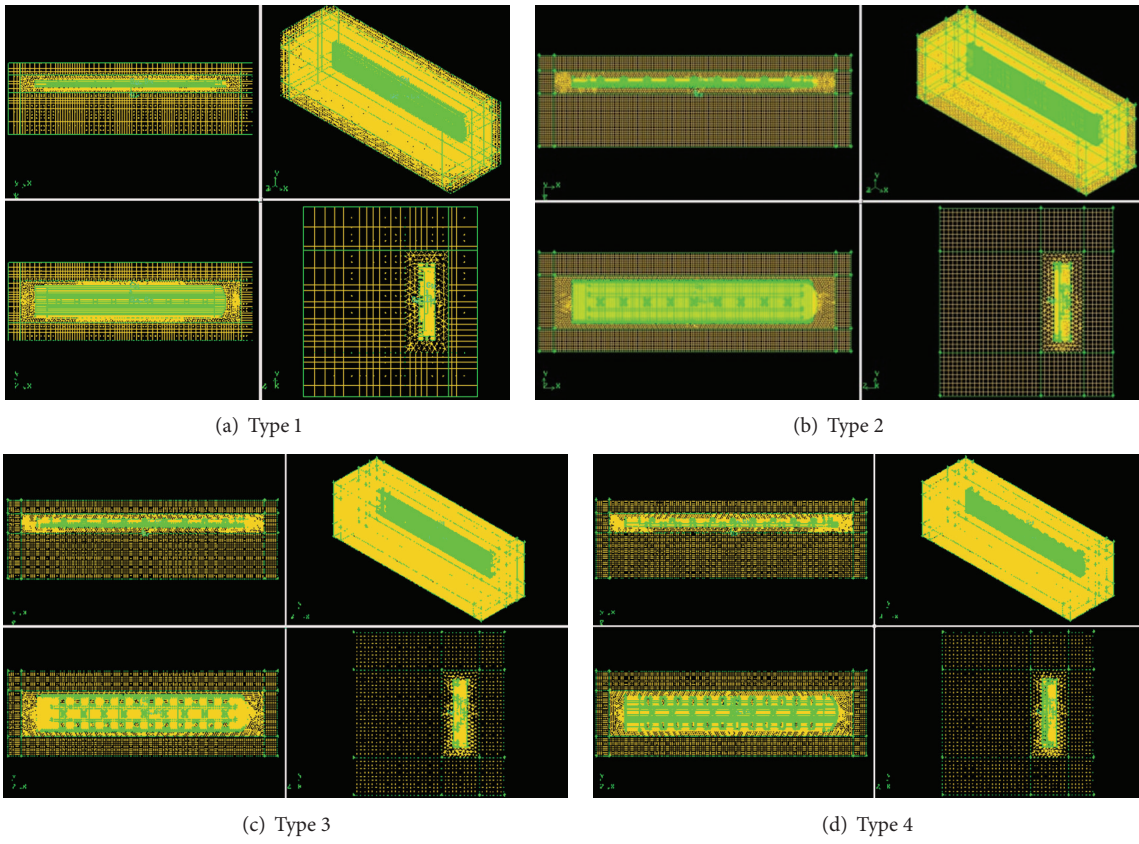


FIGURE 7: Grid structures of heat sinks.

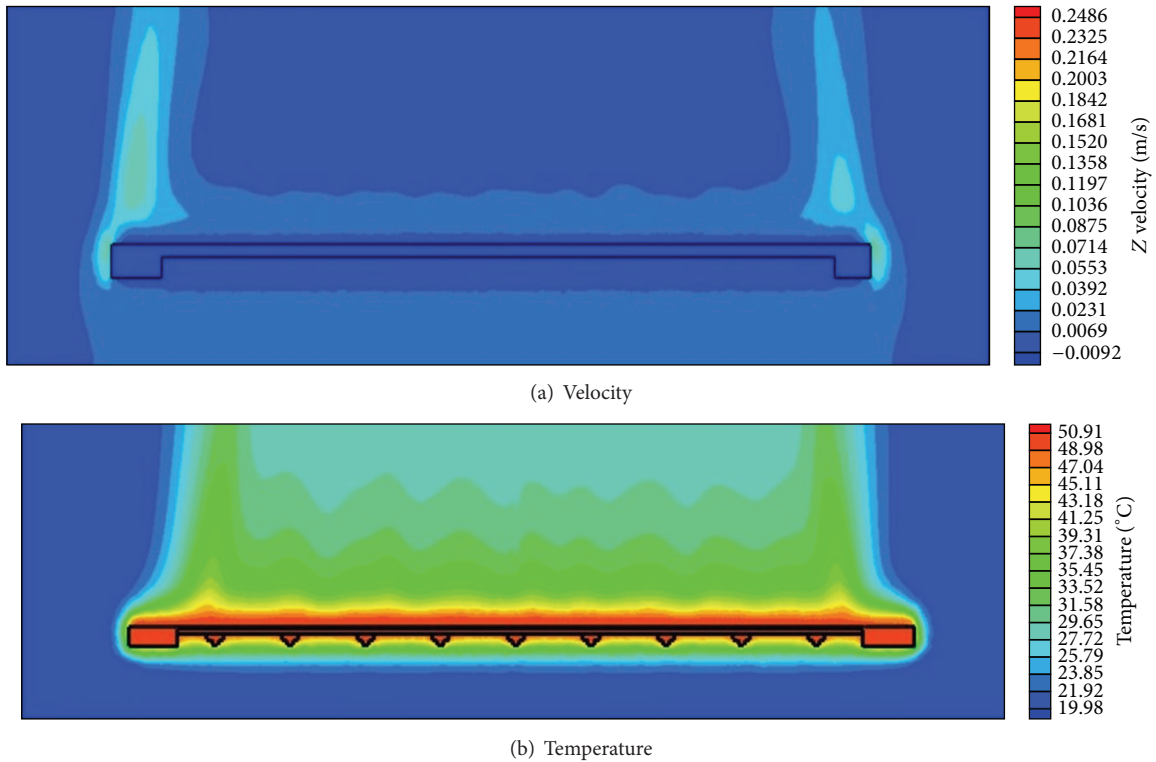


FIGURE 8: Type 1 heat sink.

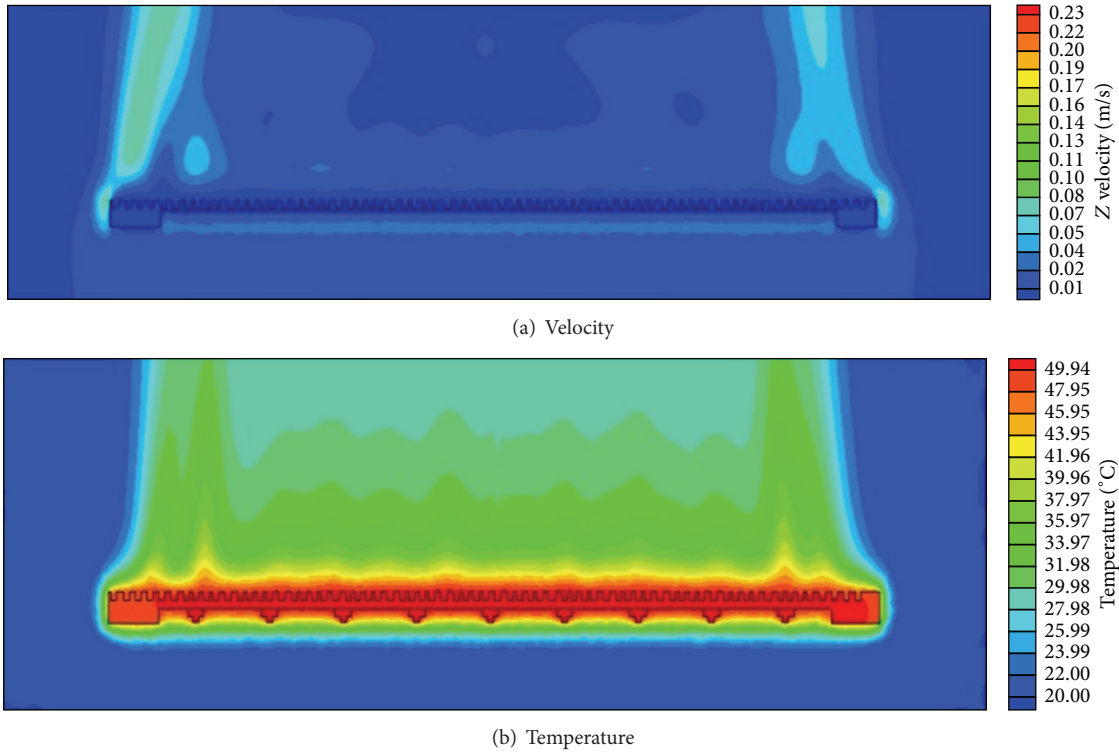


FIGURE 9: Type 2 heat sink.

TABLE 2: The error analysis of type 1 heat sink.

Monitor point	1	2	3
Experiment result (°C)	50.6	51.1	49.8
Simulation result (°C)	49.53	50.63	49.16
Error analysis (%)	2.1	1	1.3

TABLE 3: The error analysis of type 3 heat sink.

Monitor point	1	2	3
Experiment result (°C)	45.2	46.8	45.8
Simulation result (°C)	44.59	45.75	44.13
Error analysis (%)	1.3	2.2	3.6

Figure 9(a) shows the air velocity distribution around type 2 heat sink under 20°C ambient temperature. Because of larger contact areas, higher heat dissipating efficiencies can be found on both ends, which resulted in the fastest velocity (about 0.07 m/s) happening at the front and rear ends. Figure 9(b) presents the temperature distribution of type 2, which displays lower temperature in the front and rear ends and higher temperature in the middle area; the maximum overall temperature of table lamp in steady-state condition is 49.94°C. From the correlation of Figures 9(a) and 9(b), faster air velocity can be located at lower temperature area.

Although the direction of cooling fins had been changed, the heat dissipating efficiency of heat sink was not improved; therefore 12 venting holes with size of 0.8 × 1.2 × 1.2 cm ( $W \times L \times H$ ) on both outer sides of base plate were introduced, and the spacing between each hole is 1.45 cm. Since the heat released was considered only by natural convection, the air density decreased with the increasing temperature; therefore the buoyancy force occurred and generated the chimney effect eventually. This design also reduced the required

material of aluminum fins and hence reduced the weight of LED desk lamp.

Figure 10(a) shows the air velocity distribution around type 3 heat sink under 20°C ambient temperature. The influence of chimney effect results in faster velocity (0.15 m/s) which occurred in the nearby flow field. Compared with the velocities of others, type 3 is 3 times quicker than types 1 and 2. Figure 10(b) shows the temperature distribution of type 3. The figure shows that venting holes can effectively ventilate the heat away. So the maximum overall temperature of heat sink in steady-state is 46.07°C, which is lower than types 1 and 2 for about 5°C. The experiment and simulation results of type 3 are shown in Table 3; the maximum simulation error is 3.6%.

Figure 11(a) shows the velocity distribution of type 4 under 20°C ambient temperature. The velocity distribution of the transverse fins is similar with the longitudinal ones, and the faster velocity is around the venting holes. Figure 11(b) shows the temperature distribution of type 4; the maximum overall temperature of heat sink in steady-state is 45.79°C, which is lower than types 1 and 2 for

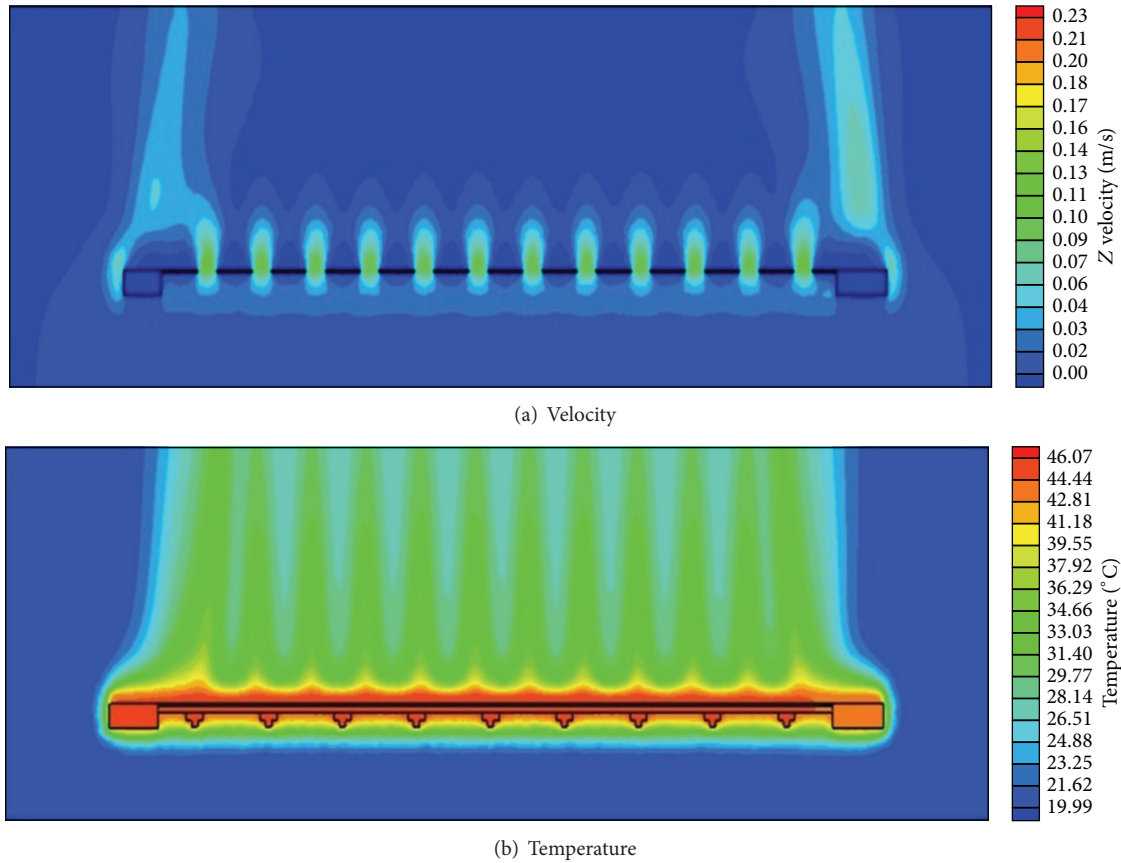


FIGURE 10: Type 3 heat sink.

about 5°C. The experiment and simulation results of type 4 are shown in Table 4; the maximum simulation error is 3%.

Compared with Figures 8(a) and 9(a), the flow rate shown in Figure 8(a) is almost zero except at both ends. Although Figure 9(a) looks similar to Figure 8(a) in the distribution of the flow field, the end flow rates of Figure 9(a) are faster. The area of heat dissipating in longitudinal fin is larger than the transverse fin, but the spacing of longitudinal fin is smaller than the transverse fin as shown in Figures 12 and 13. Such design causes longitudinal fin a poor ventilation effect and results in a poor thermal efficiency.

Compared with Figures 8(a) and 10(a), although types 1 and 3 heat sinks both possess longitudinal fins, the air flow rate around the ventilation holes is faster, which can take the heat away from the heat sink more effectively. Through the observation of temperature profiles from Figures 8(b) and 10(b), the average temperature of type 3 is smaller than type 1, which proves that an effective temperature reduction design for the LED desk lamp has been achieved.

## 5. Conclusion

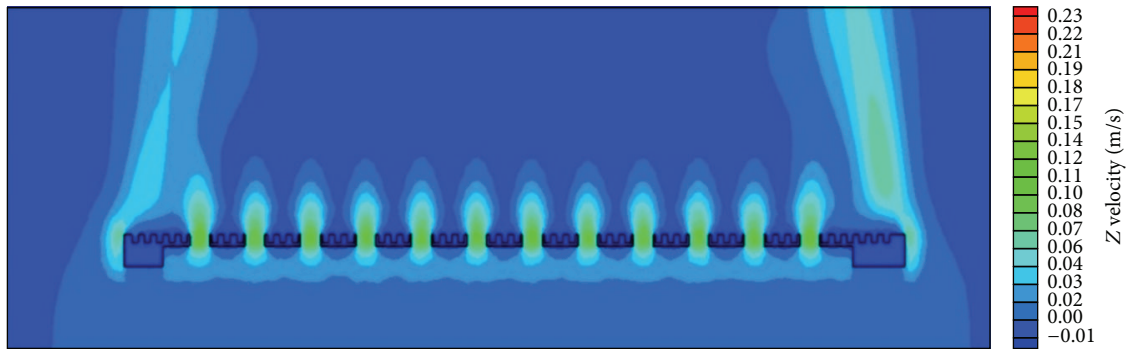
Four different types of heat sink with fins in longitudinal or transverse direction and with or without venting holes on

TABLE 4: The error analysis of type 4 heat sink.

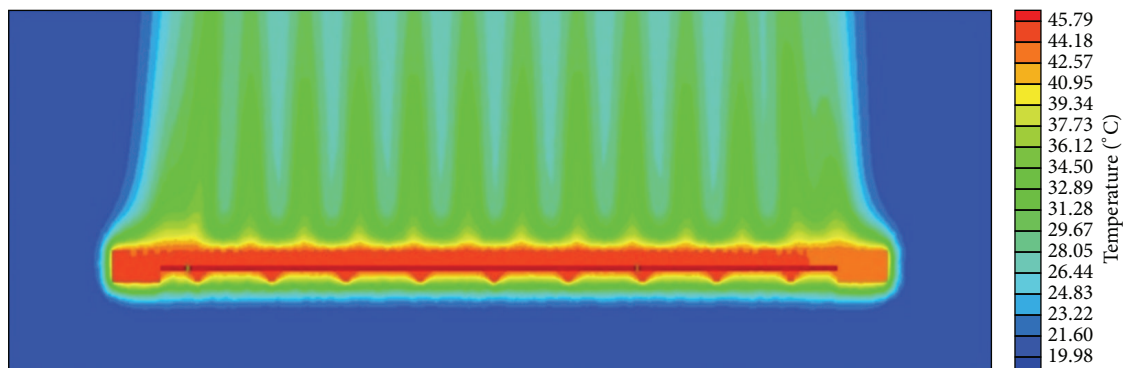
Monitor point	1	2	3
Experiment result (°C)	44.9	46.2	45.1
Simulation result (°C)	44.27	45.54	43.74
Error analysis (%)	1.4	1.6	3

base plate were compared by experiments and CFD simulations.

- (i) Under the same ambient temperature, simulation results were slightly different from the experimental results. The established CFD analysis model can reasonably predict the steady state temperature of the heat sink.
- (ii) By changing the cooling fins from transverse to longitudinal direction, the maximum temperature of heat sink dropped about 5°C from the simulation, and the maximum air flow rate increased about 0.1 m/s.
- (iii) For natural convection heat transfer, the air density decreases with the increasing temperature; hence the buoyancy force is induced. With small temperature difference, the convection phenomena are not strong enough to cause faster air flow; therefore it is hard



(a) Velocity



(b) Temperature

FIGURE 11: Type 4 heat sink.

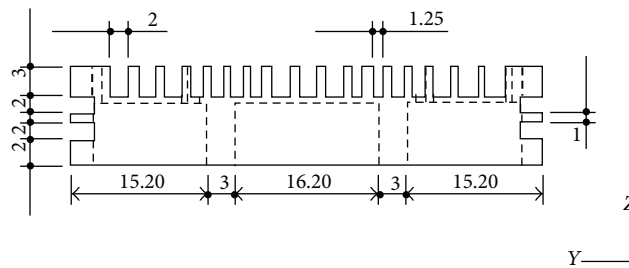


FIGURE 12: Fin spacing of types 1 and 3 heat sink (unit: mm).

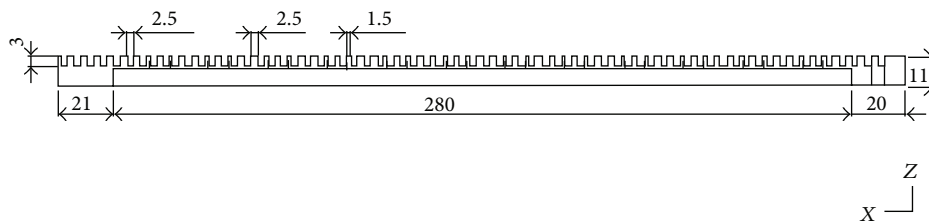


FIGURE 13: Fin spacing of types 2 and 4 heat sink (unit: mm).

to be detected in the experiment. However, the numerical simulation analysis can easily calculate and visualize the air flow rate in the overall flow field.

- (iv) An improved heat sink was designed with 12 venting holes on each outer side of base plate, by natural convection heat transfer to create the chimney effects; the air can flow quickly and a significant decrease of the maximum temperature was obtained.

## Conflict of Interests

The authors declare that there is no conflict of interests regarding the publication of this paper.

## Acknowledgment

The authors would like to express their appreciation to the Ministry of Science and Technology (NSC 101-2622-E-214-001-CC3, NSC 102-2633-E-218-001) in Taiwan for financial support.

## References

- [1] F. Wall, P. S. Martin, and G. Harbers, "High power LED package requirements," in *3rd International Conference on Solid State Lighting*, vol. 5187 of *Proceedings of the SPIE*, pp. 85–92, San Diego, Calif, USA, August 2003.
- [2] G. Harbers, W. Timmers, and W. Sillevs-Smitt, "LED backlighting for LCD HDTV," *Journal of the Society for Information Display*, vol. 10, no. 4, pp. 347–350, 2002.
- [3] H. Shaukatullah, W. R. Storr, B. J. Hansen, and M. A. Gaynes, "Design and optimization of pin fin heat sinks for low velocity applications," *IEEE Transactions on Components Packaging and Manufacturing Technology Part A*, vol. 19, no. 4, pp. 486–494, 1996.
- [4] A. De Lieto Vollaro, S. Grignaffini, and F. Gugliermetti, "Optimum design of vertical rectangular fin arrays," *International Journal of Thermal Sciences*, vol. 38, no. 6, pp. 525–529, 1999.
- [5] S.-H. Chuang, J.-S. Chiang, and Y.-M. Kuo, "Numerical simulation of heat transfer in a three-dimensional enclosure with three chips in various position arrangements," *Heat Transfer Engineering*, vol. 24, no. 2, pp. 42–59, 2003.
- [6] NICHIA, Application Note, LA-KSE3110Cm, 2003.
- [7] X. Tian, W. Chen, and J. Zhang, "Thermal design for the high-power LED lamp," *Journal of Semiconductors*, vol. 32, no. 1, Article ID 014009, 2011.
- [8] F. Harahap and D. Setio, "Correlations for heat dissipation and natural convection heat-transfer from horizontally-based, vertical-finned arrays," *Applied Energy*, vol. 69, no. 1, pp. 29–38, 2001.
- [9] S. Narasimhan and J. Majdalani, "Characterization of compact heat sink models in natural convection," *IEEE Transactions on Components and Packaging Technologies*, vol. 25, no. 1, pp. 78–86, 2002.
- [10] W. Nakayama, "Thermal management of electronic equipment: a review of technology and research topics," *Applied Mechanics Reviews*, vol. 39, no. 12, pp. 1847–1868, 1986.
- [11] J. A. Visser and D. J. de Kock, "Optimization of heat sink mass using the DYNAMIC-Q numerical optimization method," *Communications in Numerical Methods in Engineering*, vol. 18, no. 10, pp. 721–727, 2002.



# Hindawi

Submit your manuscripts at  
<http://www.hindawi.com>

